Measurement 234 (2024) 114817

Contents lists available at ScienceDirect

Measurement

journal homepage: www.elsevier.com/locate/measurement

Consumer-grade imaging system for NDVI measurement at plant scale by a farmer robot

Annalisa Milella [a,*], Giulio Reina [b]

[a] Institute of Intelligent Industrial Technologies and Systems for Advanced Manufacturing, National Research Council of Italy, via Amendola 122/D-O, Bari, 70126, Italy

[b] Department of Mechanics, Mathematics, and Management, Polytechnic University of Bari, via Orabona 4, Bari, 70125, Italy

ARTICLE INFO

Keywords:
Precision agriculture
Agricultural robotics
NDVI estimation
Plant-scale estimation
Automated in-field monitoring

ABSTRACT

The Normalized Difference Vegetation Index (NDVI) is a valuable indicator of plant vigor that is frequently used in agronomic practices to make timely and targeted decisions with the aim of increasing the productivity of the system. NDVI measurements of large-scale fields are typically performed using remote sensing from satellite and aerial imaging devices. However, due to their low spatial and temporal resolution, these technologies may have limitations in precision viticulture. This paper investigates the potential of a proximal sensing system to characterize the vine foliage that makes use of data collected by a farmer robot equipped with an Intel RealSense D435 camera. The camera includes two infrared (IR) sensors in stereoscopic configuration and one RGB sensor, which provide, for each observation, both infrared and visible red channel information, thus making possible pixel-per-pixel NDVI calculation. Solutions to IR filtering and radiometric calibration issues are proposed that significantly improve measurement accuracy and reliability. Since the camera also provides stereo-based 3D scene reconstruction, depth information can be used to separate the plant canopy from the background before NDVI measurement. At the same time, range data can be employed to extract geometric properties of the crop, such as plant height and/or volume. The system is validated in the field in a commercial vineyard at different phenological stages, from the formation of the berries to leaf discoloration and fall. Experimental results show good agreement compared with ground truth provided by a GreenSeeker, with a mean absolute percentage error in the NDVI estimation of 4.6% and a R^2 of 0.87 tested over the whole grapevine cycle. Therefore, the proposed sensing system could be a feasible solution to automated NDVI estimation at plant-scale.

1. Introduction

Quantitative metrics of plant status serve as the foundation for agronomic treatments in precision farming. Among them, the Normalized Difference Vegetation Index (NDVI) is the most widely adopted to monitor plant growth and vigor. Plants can be distinguished from other elements like soil and water by their chlorophyll, which mostly reflects near-infrared (NIR) light and absorbs red light [1]. Based on this principle, the NDVI is defined as the ratio of the difference between the reflectance in NIR and red channels, and the sum of both. Several studies have shown that the NDVI is correlated to leaf area index [2], biomass [3], plant health [4], chlorophyll and nitrogen contents [5,6].

NDVI measurements can be performed at various scales, mainly using optical devices in remote or proximal sensing configuration. While remote sensing based on multispectral or hyperspectral images from satellites and airborne devices have been in use for some decades to rapidly survey wide areas and provide prescription maps at a regional/territorial level, they generally lack the spatio-temporal resolution needed for precision farming applications. In addition, information can be affected by interference from clouds, moisture, or fog. These limitations can be overcome using unmanned aerial vehicle (UAV)-based remote sensing techniques that provide data with a ground sample distance of a few millimeters, resulting in higher spatial resolution than satellites and more flexible measurement schedules. In high-density crops, however, collecting information on biophysical properties at plant or leaf level via aerial sensing may be still infeasible. As a result, ground-based sensing has emerged as a complementary technology to provide proximal in-field measurements at a smaller scale.

In this work, a novel solution to map NDVI of vineyards by a ground robotic vehicle equipped with a consumer-grade RGB-D camera, namely the Intel RealSense D435, is proposed. This sensing device

* Corresponding author.
E-mail address: annalisa.milella@stiima.cnr.it (A. Milella).

https://doi.org/10.1016/j.measurement.2024.114817
Received 6 March 2024; Received in revised form 15 April 2024; Accepted 30 April 2024
Available online 8 May 2024

List of Acronyms

3D	Three-dimensional
CMOS	Complementary Metal-Oxide Semiconductor
Full HD	Full High Definition
GS	GreenSeeker
IR	Infrared
NDVI	Normalized Difference Vegetation Index
NIR	Near Infrared
RGB	Red Green Blue
RGB-D	Red Green Blue Depth
RGBN	Red Green Blue Near infrared
RS	RealSense
UAV	Unmanned Aerial Vehicle
UGV	Unmanned Ground Vehicle
UV	Ultra-violet
VIS	Visible
vNDVI	visible NDVI

features two infrared sensors in stereo configuration and one RGB sensor, which provide, for each point of the scene, infrared and visible information respectively thus making it possible pixel per pixel NDVI measurement. To enhance the sensor spectral response, both the IR and the RGB cameras have been endowed with optical filters to block visible and IR light respectively, attached to the camera through a 3D printed mounting case. An online radiometric calibration procedure is also proposed to convert pixel intensities to spectral reflectance values and to deal in real-time with lighting variations between subsequent images, using diffuse reflecting targets. A flowchart of the proposed approach is shown in Fig. 1, where the main steps of the processing pipeline are displayed including: 1) data acquisition, 2) plant segmentation from the overall scene based on depth data, 3) radiometric calibration for pixel to reflectance values conversion and 4) pixel per pixel NDVI calculation.

In the rest of the paper, first an overview of existing research is presented in Section 2 highlighting the main differences and advantages of the proposed system. The experimental setup and datasets are described in Section 3. Then, in Section 4, the imaging system and processing algorithms to estimate NDVI at plant scale are presented along with the radiometric calibration approach. Section 5 reports experimental results obtained for in-field tests carried out at a commercial farm. Finally, Section 6 draws the conclusions.

2. Related research

Proximal sensing has attracted increasing interest in precision farming providing in-field measurements at a smaller scale. Many active sensors have been developed [7–9], which exploit the active emission of their own light to measure the reflectance properties of the surfaces and recover reliable and consistent NDVI measurements independent of environmental lighting conditions. One of the most widely used in viticulture is the Trimble GreenSeeker. It emits brief bursts of red and infrared light and measures the amount of each type of light that is reflected back from the plant. Several works in literature have proved the effectiveness of this sensor in providing reliable information about the temporal evolution of NDVI in vineyards [10]. However, it has been shown that the measurement accuracy is sensitive to distance and orientation between the target and the measuring head of the GreenSeeker [11]. Portable field spectrometers covering a wide range of wavelengths have been also used to measure NDVI [12]. However, they are expensive and require some post-processing to recover NDVI data. In addition, portable handheld sensors may limit the automation of the data capturing process, as they generally require the intervention of human operators for accurate sensor positioning and actuation. More versatile solutions have been proposed to measure vegetation indexes using ground-based hyperspectral imaging systems, mostly set on the ground or mounted on towers [13].

Recently, standard digital RGB cameras have emerged in a number of agricultural applications including fruit counting, phenotype analysis, plant classification and disease monitoring [14]. Compared to multispectral and hyperspectral sensors, RGB cameras are less expensive and are generally easier to operate. The use of RGB cameras for the measurement of vegetation indexes in the visible spectrum has been investigated in several works. For instance, a standard RGB camera mounted on-board a UAV has been employed in [15] for calculating a visible NDVI (vNDVI), obtained with the regular RGB band values instead of the red and near-infrared bands. As an alternative, RGBN cameras have been developed to measure NDVI. RGBN cameras are obtained by removing the NIR filter typically present in standard RGB cameras in order to get information in the NIR wavelength. Hence, NDVI information can be recovered either using two-camera systems featuring a standard RGB camera for the red channel and an RGBN camera for the NIR channel or adopting a filter-switching unit, whereby the visible image and NIR images are acquired by switching the NIR rejection filter. For instance, in [16] a modified camera fitted with a near-infrared band-pass filter and a standard RGB camera mounted on a tripod are used to assess wheat status based on various vegetation indexes including the NDVI. In [17], the potential of consumer-grade standard and modified RGB cameras to measure vegetation indexes from UAVs is evaluated. Two-camera techniques allow for the simultaneous collection of information about vegetation visible and NIR properties, but they pose issues in terms of camera alignment, cross-calibration, and image capture synchronization. These issues can be avoided by alternatively applying and removing the NIR filter on a single camera, as proposed in [18] where a smartphone is used to collect first the red reflectance and then the NIR reflectance by manually adding an 800 nm high pass optical filter. A software-controlled infrared cut filter is proposed in [19], whereby a NIR filter can be switched on and off based on command scripts running on the camera. While in this case the practical limitations of manual filter removal is avoided, image matching issues may result from the time required by the filter switching mechanism, making this solution unsuitable for cameras mounted on mobile platforms.

In any of the cases above, NDVI estimates are either performed remotely based on aerial vehicles or rely on ground-based measures using fixed installations or handheld devices. More recently, Unmanned Ground Vehicles (UGVs) and conventional tractors equipped with imaging sensors have been proposed as a complementary solution to collect high resolution proximal data and provide information on plant characteristics at centimeter or sub-centimeter scale. While much work has been done for applications such as fruit detection and counting [20,21], only a few examples exist in the context of foliage characterization. A first attempt can be found in [22], where a methodology to generate globally-referenced vigor maps in vineyards from ground images taken with a camera mounted on a conventional tractor is proposed. It uses a monocular camera able to sense in the visible, NIR, and UV spectra, selectively isolated with bandpass filters. In [23], a multispectral camera mounted on a tractor is proposed to estimate NDVI in vineyards and results are compared with GreenSeeker measurements. A radiometric calibration approach is used which exploits a MacBeth color chart to transform pixel intensities to reflectance values. A wide black panel is attached to the tractor through a metallic frame as background screen to ease canopy segmentation. A red-edge multi-spectral camera mounted on-board a farmer robot is also used in [24] to gather NDVI measurements in vineyards. A sensing system for an autonomous scouting robot, using artificial lighting and a hyperspectral camera, is

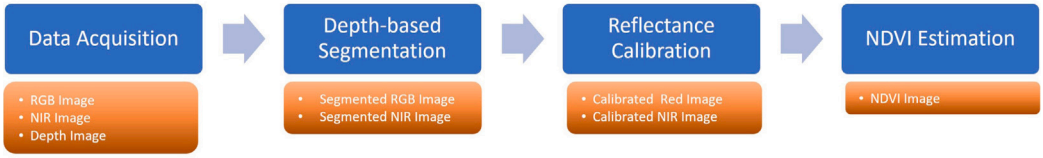

Fig. 1. Flowchart of the proposed approach for NDVI estimation.

developed in [25] to automatically acquire spectral reflection data and measure NDVI in soybean fields at night.

A novel approach is proposed in this research where NDVI map of vineyards is obtained by a ground robotic vehicle equipped with a consumer-grade RGB-D Intel RealSense D435. Since this device includes two distinct sensors to provide visible and infrared images, the proposed system can be classified as a two-camera solution. However, unlike typical two-camera systems, it features a built-in structure in which all sensors are spatially and timely synchronized, hence overcoming image matching issues. As an additional advantage, the sensing device also provides depth information, which can be exploited to ease plant segmentation from the background, avoiding the need for complex data processing or bulky background screens. The proposed approach is validated in the field at different phenological stages, showing good agreement with measurements provided by a GreenSeeker. It is worth noticing that the sensing system has a total cost of about 0.4k euros for the camera and the optical filters that is lower than the Greenseeker (1k euros) and about forty times less expensive than a standard multispectral camera. An additional cost of about 0.9k euros should be considered for the calibration targets that however are required by multispectral approaches as well. Furthermore, the camera's ability to generate 3D data allows for simultaneous measurement of plant morphological traits like height and volume [26]. This source of information is not available either with the Greenseeker or the multispectral camera. Hence, the proposed system could be a viable and cost-effective solution to provide information on individual plant development and health status.

In summary, the main contributions of this research are:

- the development of a proximal sensing system for NDVI estimation using an Intel RealSense D435 camera, enhanced with IR optical filters. This system provides a feasible measurement device that can be easily integrated onboard agricultural vehicles or deployed manually. The use of the RealSense camera in agricultural applications has been recently demonstrated for tasks including crop reconstruction and fruit detection, and for robot navigation purposes. To the best of our knowledge, this is the first research investigating the potential of a RealSense camera for NDVI measurement at plant scale by a farmer robot;
- a novel online radiometric calibration procedure to deal with uncontrolled and rapidly changing lighting conditions, based on calibration targets integrated with the camera system. This allows for online estimation of the calibration at every new image acquisition, which can be used to convert image pixel values into reflectance values ensuring consistent NDVI measures;
- a robotic platform for automated in-field monitoring and characterization at plant scale in viticulture. The platform is also equipped with an accurate GPS-based localization system that can be used in conjunction with the imaging device to get high-resolution NDVI maps.

3. Materials

3.1. Robotic acquisition system

For in-field data collection, a custom-built farmer robot named Polibot (see Fig. 2(a)) is employed. The farmer robot is designed to provide mobility over highly irregular terrain [27], by leveraging on an articulated suspension system that can handle high payload, ensure vibration isolation, and navigate agricultural terrain similarly to a multi-legged insect. The control and acquisition systems are implemented using the Robot Operating System (ROS), which provides a versatile and robust operating foundation. The robot is outfitted with an Intel RealSense D435 imaging device (Santa Clara, CA, USA), which is used to capture RGB, infrared and depth data. It consists of a color camera and a stereo pair of infrared (IR) cameras that offer depth information. The stereo imagers feature a field of view of 87(H) × 58(V) deg, maximum depth resolution of 1280 × 720 px, and frame rate up to 90 fps, with an ideal perception range of 0.3 m up to 3 m. The IR stereo stream is spatially calibrated and time synchronized with the color stream provided by a Full HD (1920 × 1080) CMOS camera, with nominal field of view of 69(H) × 42(V) deg and a maximum frame rate of 30 fps at full resolution. To enhance IR images and depth reconstruction, a Quanmin 9.6 mm × 1.0 mm Slim Optical 780 nm cold mirror filter was added in front of each IR sensors to cut visible light. As the RGB camera has no built-in IR-cut filter, a Gzikai 650 nm 10 mm × 1 mm UV-IR Cut Filter was also positioned in front of the RGB sensor. All filters were mounted on a custom-built support made by 3D printing, as shown in Fig. 2(c). The camera was mounted on an aluminum frame and attached to the robot, angled by 90 degrees to collect data in portrait mode.

A close-up of the setup for adaptive radiometric calibration of the sensors is shown in Fig. 2(b). It consists of two Optopolymer calibrated reflectance standards with 5% and 70% reflectance grades, respectively, which were positioned on a metal frame so that both targets are always visible in the lower section of all captured images (both RGB and NIR). A sample acquisition result is reported in Fig. 3, showing from left to right the RGB image, the left IR image and the depth image. As will be detailed in the following, the RGB and left IR images are used for NDVI estimation, whereas the depth image is employed to separate the plant row from the background by setting a distance range. In addition, the robotic platform is equipped with an accurate localization system using a dual GPS configuration [28] that can work in conjunction with the imaging device to get geo-referenced NDVI information.

3.2. Datasets

Data collection was performed in a commercial vineyard located in San Donaci (BR), Italy, with grape variety Vitis vinifera, cultivar "Negroamaro" (red grape variety). The available experimental test site included three vine rows, each one comprising about 100 plants, covering a total area of approximately 0.1 ha. A Google Earth view of the test site is shown in Fig. 4, with the experimental region highlighted by a yellow box. Images were acquired at a frame rate of 6 Hz and at a distance of about 1 m from the row canopy. Four datasets were collected in 2023, spanning three stages of grapevine phenological development, from berry formation and development(June–July), to the end of grape ripening (September) and after harvesting at the beginning of leaf discoloration and fall (October). More than 37.000 RGB images and corresponding NIR images with 1280 × 720 pixel resolution were collected (see Table 1). All acquisitions were mostly performed around the zenith time to optimize image quality and reduce visual artifacts and shadows. Sky conditions varied from fully sunny to partially or mostly cloudy. The rows were scanned on both

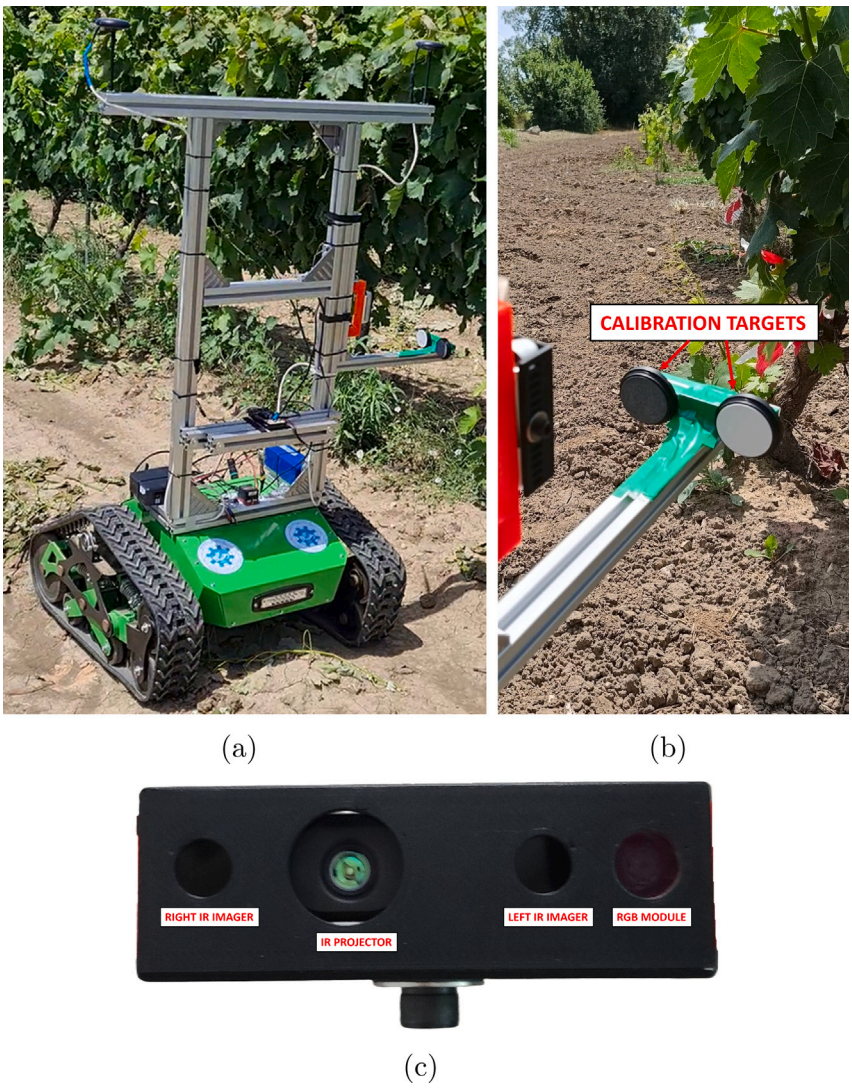

Fig. 2. Acquisition system: (a) robotic platform; (b) calibration system using Optopolymer calibrated reflectance targets; (c) Intel RealSense D435 enhanced with two cold mirror filters (applied to the left and right infrared imagers) and an IR-cut filter (applied to the RGB module). The RealSense camera also includes an IR projector, which was kept off during the experiments.

sides. This resulted in a high level of heterogeneity in the dataset. Due to such variability, exposure and white balance were set in auto mode.

Image acquisitions performed with the RealSense were paired with measurements from a Trimble GreenSeeker handheld sensor. GreenSeeker measurements were collected for one of every six plants leading to around 17 measurements per row, recorded with the smartphone GreenSeeker BT Logger V 1.0 app. The GreenSeeker emits brief bursts of red (650 nm) and infrared (770 nm) light and then returns the amount of each type of light that is reflected back from the plant in terms of an NDVI reading (ranging from 0.00 to 0.99) on its LCD display screen. It is worth to note that the GreenSeeker works within a distance range of 60–120 cm, with a wider field of view the greater the distance from the object of interest. Given this constraint and the camera field of view, the GreenSeeker acquisitions were performed by manually positioning the sensor at about 1 m from the plant with a viewing direction orthogonal to the plant canopy extension. This assured that both the GreenSeeker and the RealSense were looking approximately at the same area.

4. Methods

4.1. Adaptive radiometric calibration

During the field experiments, lighting variations between images of the same dataset can be observed. Such changing conditions prevent their consistent comparison to determine the physiological status of vegetation. Therefore, an adaptive radiometric calibration procedure is proposed. It allows images to be calibrated in reflectance, using two calibrated targets always visible in the camera field of view as previously described in Section 3.1. For each spectral channel, a linear regression can be established between pixel values (p) of the calibration targets expressed in the range (0–255) and their reflectance (ρ_{ch}) as [30]:

$$\rho_{ch} = a^I_{ch} p + b^I_{ch} \tag{1}$$

where (a^I_{ch}, b^I_{ch}) are the parameters of the linear equation for each channel ch (red and NIR) of image I. Note that since the targets are mounted on an aluminum bar attached at a fixed position with respect to the camera, the image region occupied by the targets (i.e., lower

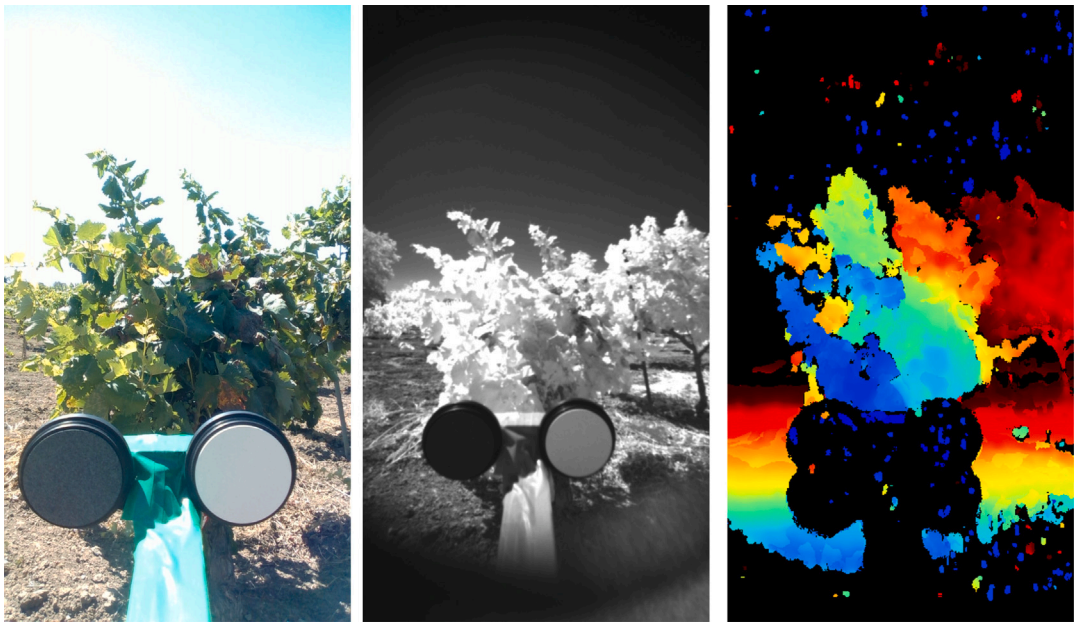

Fig. 3. Sample images acquired in the field. From left to right: color, left infrared and depth image.

Fig. 4. Google Earth view of the test site in San Donaci (BR), Italy. The experimental field, including three crop rows (marked as 1-2-3), is highlighted by a yellow box. The length of each row is of about 100 m and the covered area is approximately of 0.1 ha. Each row was scanned by both sides (A,B).

Table 1
Datasets acquired in 2023 from the beginning of berry formation to leaf discoloration and fall.

Datasets	N.1	N.2	N.3	N.4	N.5
Date	06/06/2023	06/21/2023	07/27/2023	09/14/2023	10/19/2023
Hour (CEST)	11:00-12:00	10:00-11:00	10:00-11:00	11:15-12:15	11:00-12:00
Phenological Stage [29]	Pea-sized berries (75)	Berries beginning to touch (77)	Beginning of ripening (81)	Berries ripe for harvest (89)	Beginning of leaf discoloration and fall (92-93)
Nr. of images per channel	6234	5118	6522	12 660	7074

part of the field of view) is fixed and can be defined once at the beginning of operation. Calibration parameters can be then recalculated at every new image acquisition and used to convert image pixel values into reflectance values for successive NDVI computation according to Eq. (1), as will be described in the following.

4.2. Image processing for NDVI calculation

A method to estimate NDVI from images acquired by the Intel RealSense sensor is proposed. The NDVI is based on the principle that chlorophyll absorbs visible light for photosynthesis, while the cell structure of leaves strongly reflects near-infrared light. The NDVI is defined as:

$$NDVI = \frac{NIR - VIS}{NIR + VIS} \tag{2}$$

where VIS and NIR stand for the spectral reflectance measurements acquired in the visible (red) and near-infrared regions, respectively. The NDVI ranges between −1 and 1. Healthy plants typically generate high NDVI (0.6 or greater) and in the other case, the index is between 0 and 0.3. Lifeless zones produce low results (lower or equal to 0).

The first step necessary to calculate the NDVI index from images acquired by the RealSense is to separate the plant from the background. Segmentation is especially critical for plants that have low foliage density as vineyards, since in this case it is necessary to single out the

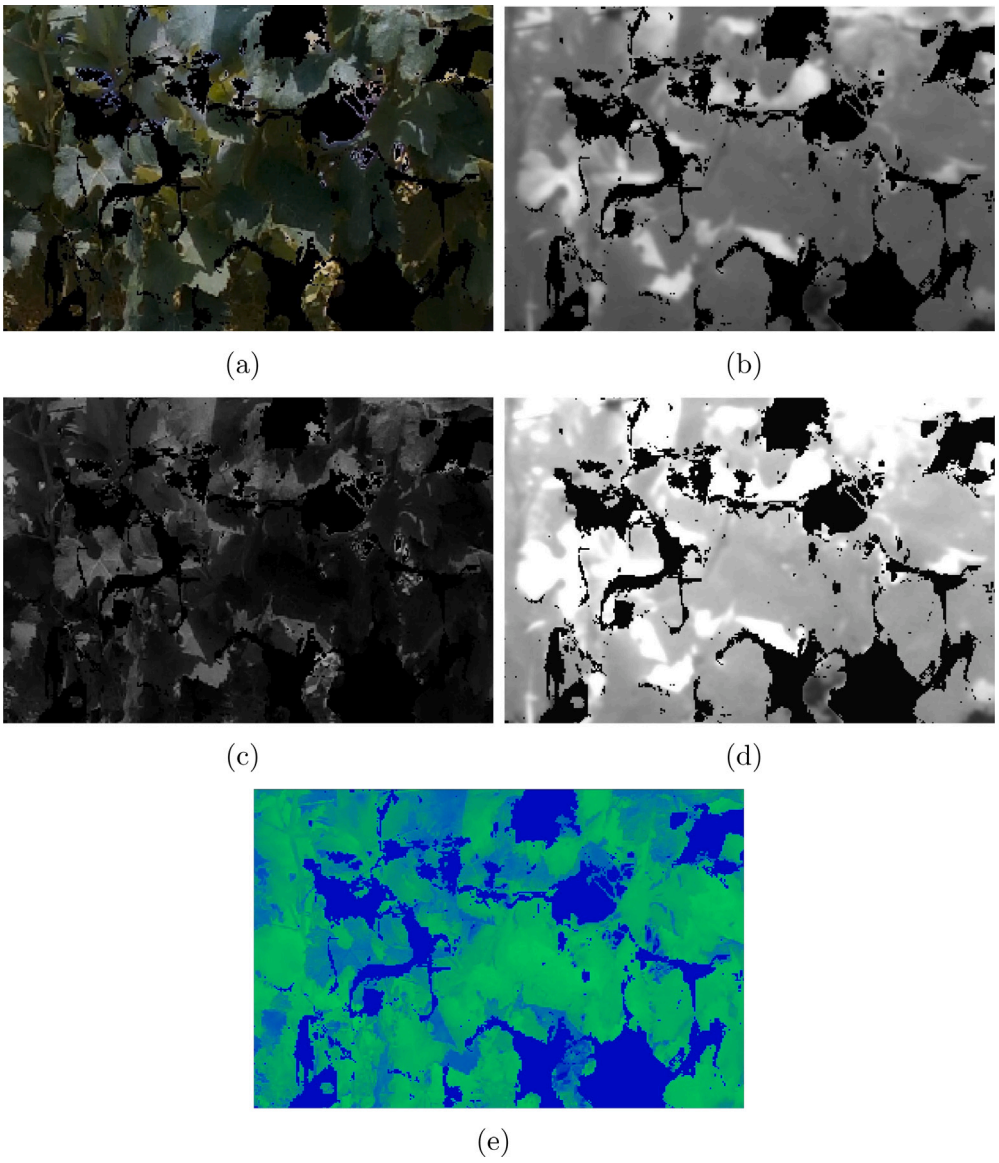

Fig. 5. Image processing steps for NDVI estimation for a sample case. (a) Segmented color image aligned to depth geometry; (b) segmented left NIR image; (c)–(d) reflectance images after radiometric calibration for the red and NIR channels, respectively; (e) NDVI image with greener points corresponding to higher NDVI values.

canopy from the background that may cover a large image portion and involve regions that are far away from the surveyed plant. To this end, depth information is used to select only the points that fall within a certain distance range from the camera in both the color and the IR image. While more sophisticated solutions using semantic segmentation techniques may be used without modifying the overall framework of the proposed system, distance-based segmentation was found to work well for our purposes. In this respect, it should be noted that since the lower part of the camera field of view is occluded by the calibration targets, only the upper part of the image needs to be processed (see Fig. 3 as an example). In addition, a 40 cm wide Region of Interest (ROI) corresponding approximately to the GreenSeeker reading area is set in the vegetation area to compute NDVI values. Indeed, depth-based segmentation does not allow for separation of branches, poles and wires lying in the vicinity of the canopy, which are therefore included in the vision-based estimates. However, it is worth noting that branches and other wooden or support structures close to the canopy are not excluded from GreenSeeker field of view either.

Once the ROI has been selected in both the color and NIR images, the red and NIR channels are calibrated in reflectance following the procedure described in Section 4.1. Then, for each segmented scene point, the reflectance value in the red image and the corresponding value in the NIR image are collected and used for pixel per pixel NDVI computation. The average of all NDVI values for the single image is finally calculated and used for comparison with the GreenSeeker measurement for the same plant. As an example, Fig. 5 illustrates the steps of the image processing pipeline for a test case. Specifically, Fig. 5(a)–(b) show the results of segmentation for the color and NIR images in the selected ROIs, respectively. The red and NIR channels after radiometric calibration are displayed in Fig. 5(c)–(d). The resulting NDVI image is shown in Fig. 5(e).

Table 2
Accuracy of the proposed approach using the RealSense (RS) camera with respect to GreenSeeker expressed in terms of Mean Absolute Percentage Error ($MAPE$), standard deviation (σ) and maximum error ($maxPE$) for both the calibrated and uncalibrated case.

	$MAPE_{\%}$	$\sigma_{\%}$	$maxPE_{\%}$
Calibrated RS	4.6	2.0	8.7
Uncalibrated RS	16.4	5.9	25.7

Fig. 6. RGB images of a plant of row 1-A during the different phenological stages. The NDVI value estimated by the proposed approach is overlaid on each image.

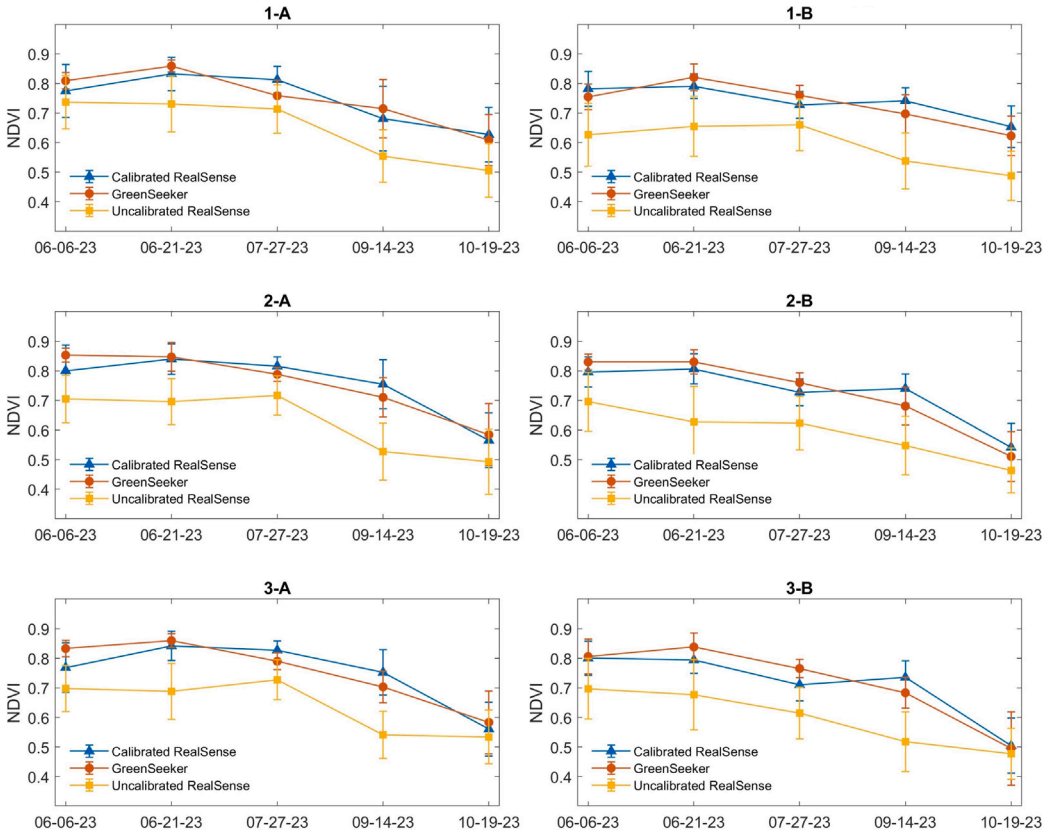

Fig. 7. Temporal evolution of the NDVI as estimated by the calibrated RealSense camera, the uncalibrated RealSense camera and the GreenSeeker for each row (1-2-3) scanned from both sides (A–B).

5. Results and discussion

The temporal evolution of the NDVI was analyzed as a function of the phenological stage. As an example, RealSense NDVI estimates are reported in Fig. 6 for a plant of row 1, inspected from side A during the different plant development phases. As apparent from this figure, the NDVI increases during the summer months, reaching its peak at the end of July. It inverts its trend in September with a significant drop after the harvesting stage in mid October.

The evolution of the average NDVI values along all rows of the experimental test site scanned on either side over the course of the phenological stages is shown in Fig. 7. Specifically, results from both calibrated and uncalibrated images (i.e., using pixel values instead of reflectance values) are reported and compared with GreenSeeker measurements. It can be noticed that all curves show similar outcome with a decreasing trend of the NDVI from berry formation (June) to leaf fall (October). The discrepancy between the RealSense camera and the GreenSeeker measurements can be expressed in terms of absolute percentage error (PE_i) as:

$$PE_i = \left| \frac{NDVI^i_{RS} - NDVI^i_{GS}}{NDVI^i_{GS}} \right| \times 100 \tag{3}$$

where $NDVI^i_{RS}$ is the average NDVI estimate provided by the proposed approach using the RealSense camera and $NDVI^i_{GS}$ is the average measurement provided by the GreenSeeker along a given crop row i, with $i = 1, 2, 3$.

Numerical results are collected in Table 2. Specifically, considering all PE_i, the Mean Absolute Percentage Error ($MAPE$), the standard deviation σ and the maximum error ($maxPE$) are reported for both the calibrated and uncalibrated case. It can be seen that using the calibrated camera a MAPE of 4.6% with standard deviation of 2.0% and a maximum absolute percentage error of 8.7% are found, which demonstrate a good agreement between the two sensing devices. For the calibrated case, individual PE_i values are also illustrated in Fig. 8 in the form of a bar graph. Results are further confirmed in Fig. 9, showing good correlation between the calibrated RealSense and the GreenSeeker measurements with a correlation coefficient R^2 of 0.87.

The calibration system proves to be critical for the accuracy of the vision-based measurement approach. For the uncalibrated imaging approach, the MAPE increases to 16.4% with a standard deviation of 5.9% and maximum error of 25.7% as indicated in Table 2. Nevertheless, the measurements are still well correlated with R^2 of 0.74, as can be seen by the correlation graph reported in Fig. 10. It should be also

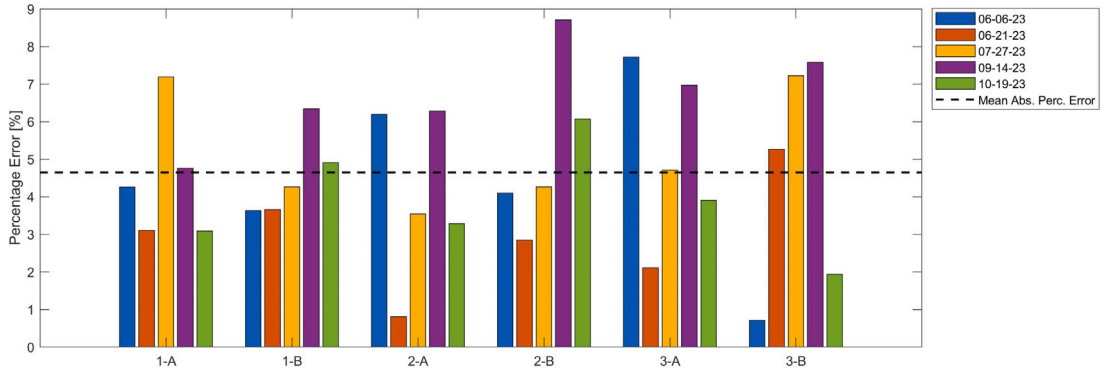

Fig. 8. Absolute percentage errors PE_i, shown as a bar graph. Each bar of the plot represents the absolute percentage error between of the average NDVI returned by the calibrated RealSense camera and the GreenSeeker for a given row (i=1,2,3) scanned by side A or B at a given phenological stage. The MAPE calculated over all measurements is also displayed as a black dashed line.

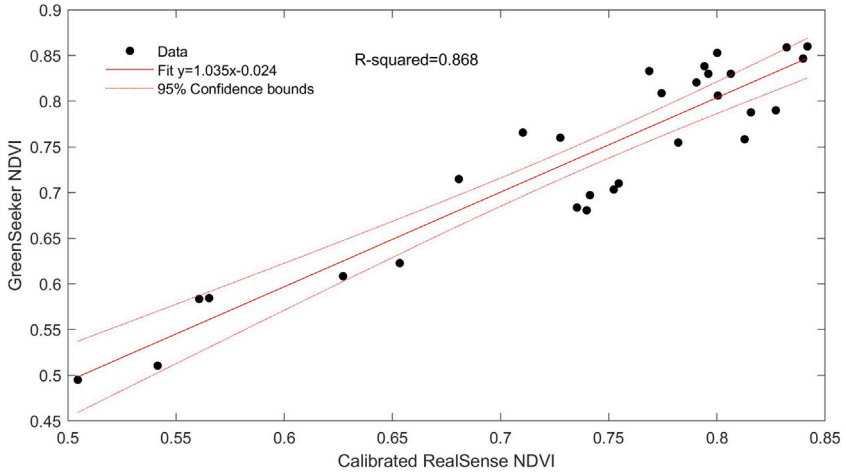

Fig. 9. Correlation between calibrated RealSense and GreenSeeker NDVI measurements.

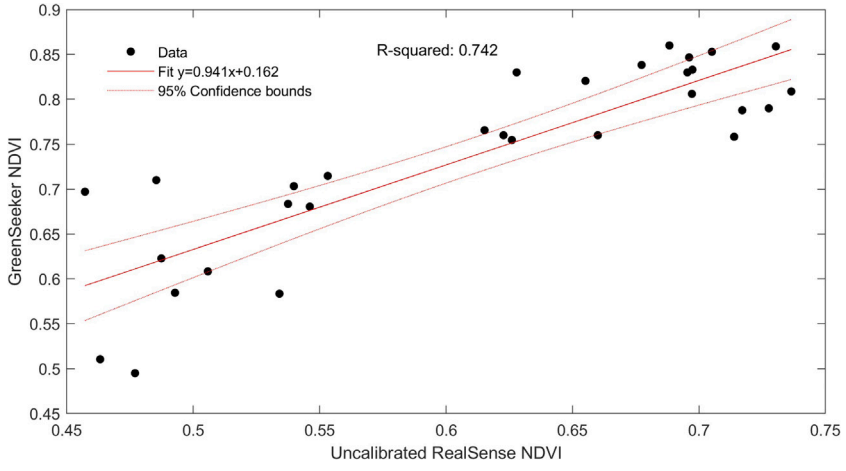

Fig. 10. Correlation between uncalibrated RealSense and GreenSeeker NDVI measurements.

noticed that although each single experiment extends over a relatively short path (around 100 m) and time (approximately 3 min), significant changes in environmental lighting conditions were observed. Hence, calibration parameters changed from one image to another. As an example, the distribution of the calibration parameters (see Eq. (1)) for one field test is shown in the box plots of Fig. 11 for the red and NIR channel.

Results reported so far have demonstrated the capability of the proposed system of capturing the temporal evolution of the NDVI in the field at row level. However, the system is able to perform geo-referenced localized measures at plant/leaf level as illustrated in Fig. 12 for one of the test rows. This allows for identifying, where needed, attention spots (i.e., points with lower NDVI values like P1, P2, P3) also retrieving the corresponding visual images for further inspection. In

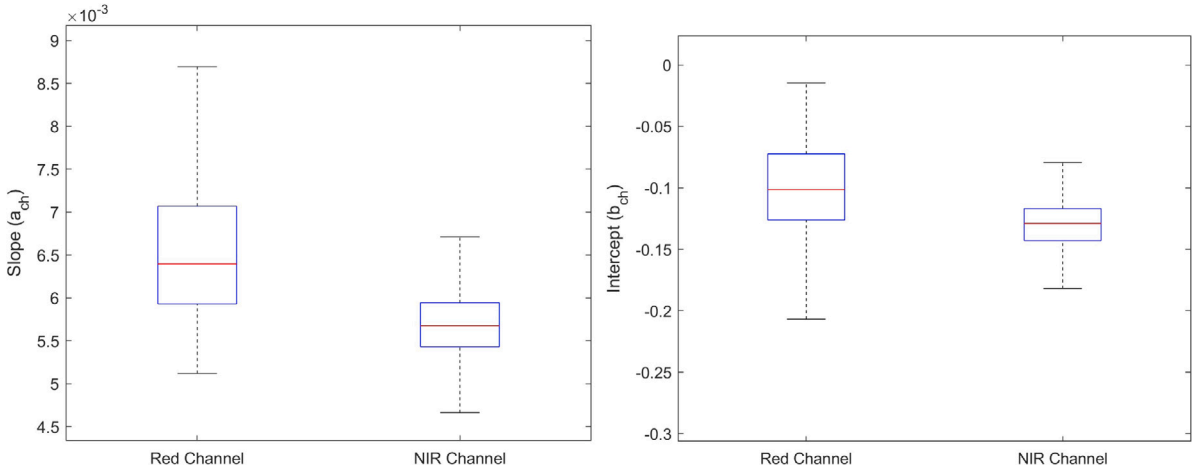

Fig. 11. Variation of calibration parameters for one field test. On each box, the central red line indicates the median, and the bottom and top edges of the box indicate the 25th and 75th percentiles, respectively. The whiskers extend to the most extreme data points excluding outliers.

Fig. 12. Google Earth projection of NDVI measurements (displayed in winter color map) along row 1 inspected from side B, with greener points denoting higher NDVI values. Attention spots (points with lower NDVI such as P1, P2, P3) can be easily detected and the corresponding images retrieved for further inspection.

particular, the analysis of the depth-aligned color images in proximity of the point P3 reveals the absence of vegetation as shown in Fig. 13. This highlights an additional advantage of the proposed technology, that is the possibility of estimating plant vigor based on appearance information (i.e., color and NIR data) and to measure at the same time morphological characteristics, such as plant height or foliage density, based on 3D data.

6. Conclusion

In this work, the potential of an Intel RealSense D435 camera mounted onboard a farmer robot in estimating NDVI in vineyards was investigated. The camera was enhanced with optical filters to improve the output signals from both the infrared and visual sensor. In addition, an online radiometric calibration approach was proposed to deal with lighting variations and transform pixel intensities into reflectance values. The NDVI was measured, pixel per pixel, using data from both near-infrared and red light reflected from the acquired scene and compared with measurements provided by a Trimble GreenSeeker. Experimental tests were performed in a Negroamaro commercial vineyard over multiple phenological stages from berry formation to leaf discoloration and fall with the following main findings:

- good accuracy performance with a mean percentage error of 4.6% and a correlation coefficient R^2= 0.87 between RealSense and GreenSeeker records;
- the online radiometric calibration system was critical to deal with uncontrolled lighting variations and ensure consistent and accurate results;
- the use of an RGB-D sensing device allows for the simultaneous availability of depth data that can ease image segmentation and provide additional information on plant status based on morphological characteristics, such as plant height or volume;
- the camera was integrated onboard a farmer robot to map NDVI measurements along a vineyard row, showing that the proposed system provides a useful technology for in-field close range monitoring of crop growth and health status.

It should be noticed that the use of a consumer-grade camera fulfills the two requirements of cost-effectiveness (< 400 Euros) and user-friendliness (thanks to the availability of the open-source Intel SDK). The camera can be mounted onboard a farmer robot or any other agricultural vehicle. It can also be used in a ground-based or handheld configuration. In addition, the proposed processing pipeline does not involve computationally expensive algorithms and it can run real-time

Fig. 13. Image sequence in proximity of position P3: original color images (up) and depth-based segmented images (bottom). In this case, depth-based segmentation points out a region with low foliage occupation (plants on the background are filtered out based on distance information). Hence, the system can simultaneously capture appearance and morphological characteristics of the crop, based on RGB-NIR and depth data, respectively.

on standard or embedded computers. As such, the proposed system could contribute to make robotic technology more accessible to traditional farming environments, making farming more attractive for the young and tech-affine generation, and thus counteracting the emerging shortage of young, skilled workers.

The current study was performed on a single grape variety and a relatively limited field extension. Given the promising results, future research efforts will be devoted to the validation of the system in different vine cultivars as well as other vegetation species. The influence of lighting conditions (e.g., sun-angle variations) and of the camera position with respect to the canopy will also be specifically investigated. In addition, the use of different optical filter combinations to further improve the output signals from both the IR and visual sensor will be researched. The combined use of depth and color information to enhance image segmentation and reduce the influence on the measurement of non-vegetative areas will be an additional focus of the research. The comparison with multispectral or hyperspectral imaging devices will be performed to further verify the potential and reliability of the proposed system.

CRediT authorship contribution statement

Annalisa Milella: Writing – review & editing, Writing – original draft, Validation, Software, Methodology, Investigation, Funding acquisition, Formal analysis, Data curation, Conceptualization. **Giulio Reina:** Writing – review & editing, Writing – original draft, Validation, Supervision, Methodology, Investigation, Funding acquisition, Formal analysis, Conceptualization.

Declaration of competing interest

The authors declare that they have no known competing financial interests or personal relationships that could have appeared to influence the work reported in this paper.

Data availability

Data will be made available on request.

Acknowledgments

This work was partially funded by the following projects: Agricultural inTeroperabiLity and Analysis System (ATLAS), H2020 (Grant No. 857125); E-crops - Technologies for Digital and Sustainable Agriculture, Italian Ministry of University and Research (MUR) under the PON Agrifood Program (No. ARS01_01136); giving Smell sense To Agricultural Robotics (STAR), ERA-NET COFUND ICT AGRI-FOOD (Grant No. 45207); CNR DIITET project DIT.AD022.207, STRIVE-le Scienze per le TRansizioni Industriale, Verde ed Energetica (FOE 2022), sub-task activity Agro-Sensing2. The authors are grateful to Cantina San Donaci agricultural farm for hosting experimental tests in the context of the E-Crops project.

References

[1] S.L. Ustin, S. Jacquemoud, How the optical properties of leaves modify the absorption and scattering of energy and enhance leaf functionality, in: J.

Cavender-Bares, J.A. Gamon, P.A. Townsend (Eds.), Remote Sensing of Plant Biodiversity, Springer International Publishing, Cham, 2020, pp. 349–384, http://dx.doi.org/10.1007/978-3-030-33157-3_14.

[2] L. Johnson, D. Roczen, S. Youkhana, R. Nemani, D. Bosch, Mapping vineyard leaf area with multispectral satellite imagery, Comput. Electron. Agric. 38 (1) (2003) 33–44, http://dx.doi.org/10.1016/S0168-1699(02)00106-0.

[3] G.D. Farias, C. Bremm, C. Bredemeier, J. de Lima Menezes, L.A. Alves, T. Tiecher, A.P. Martins, G.P. Fioravanço, G.P. da Silva, P.C. de Faccio Carvalho, Normalized Difference Vegetation Index (NDVI) for soybean biomass and nutrient uptake estimation in response to production systems and fertilization strategies, Front. Sustain. Food Syst. 6 (2023) http://dx.doi.org/10.3389/fsufs.2022.959681.

[4] S. Di Gennaro, E. Battiston, S. Di Marco, O. Facini, A. Matese, M. Nocentini, A. Palliotti, L. Mugnai, Unmanned Aerial Vehicle (UAV)-based remote sensing to monitor grapevine leaf stripe disease within a vineyard affected by esca complex, Phytopathol. Mediterr. 55 (2) (2016) 262–275, http://dx.doi.org/10.14601/Phytopathol_Mediterr-18312.

[5] G. Caruso, G. Palai, L. Tozzini, C. D'Onofrio, R. Gucci, The role of LAI and leaf chlorophyll on NDVI estimated by UAV in grapevine canopies, Sci. Hort. 322 (2023) 112398, http://dx.doi.org/10.1016/j.scienta.2023.112398.

[6] B. Mitra, P. Singha, A. Roy Chowdhury, A.K. Sinha, M. Skalicky, M. Brestic, S. Alamri, A. Hossain, Normalized difference vegetation index sensor-based nitrogen management in bread wheat (*Triticum aestivum L.*): Nutrient uptake, use efficiency, and partial nutrient balance, Front. Plant Sci. 14 (2023) http://dx.doi.org/10.3389/fpls.2023.1153500.

[7] L.K. Sharma, H. Bu, A. Denton, D.W. Franzen, Active-optical sensors using red NDVI compared to red edge NDVI for prediction of corn grain yield in North Dakota, U.S.A., Sensors 15 (11) (2015) 27832–27853, http://dx.doi.org/10.3390/s151127832.

[8] J. Lu, Y. Miao, W. Shi, J. Li, F. Yuan, Evaluating different approaches to non-destructive nitrogen status diagnosis of rice using portable RapidSCAN active canopy sensor, Sci. Rep. 7 (2017) 14073, http://dx.doi.org/10.1038/s41598-017-14597-1.

[9] M.M. Conley, A.L. Thompson, R. Hejl, Proximal active optical sensing operational improvement for research using the CropCircle ACS-470, implications for measurement of Normalized Difference Vegetation Index (NDVI), Sensors 23 (11) (2023) http://dx.doi.org/10.3390/s23115044.

[10] A. Junges, D. Fontana, R. Anzanello, C. Bremm, Normalized difference vegetation index obtained by ground-based remote sensing to characterize vine cycle in Rio Grande do Sul, Brazil, Ciência Agrotecnologia 41 (2017) 543–553, http://dx.doi.org/10.1590/1413-70542017415049016.

[11] D.E. Martin, J.D. Lopez Jr., Y. Lan, Laboratory evaluation of the GreenSeeker handheld optical sensor to variations in orientation and height above canopy, Int. J. Agric. Biol. Eng. 5 (2012) http://dx.doi.org/10.3965/j.ijabe.20120501.005.

[12] B. Baca-Bocanegra, J.M. Hernández-Hierro, J. Nogales-Bueno, F.J. Heredia, Feasibility study on the use of a portable micro near infrared spectroscopy device for the "in vineyard" screening of extractable polyphenols in red grape skins, Talanta 192 (2019) 353–359, http://dx.doi.org/10.1016/j.talanta.2018.09.057.

[13] X. Ye, K. Sakai, H. Okamoto, L.O. Garciano, A ground-based hyperspectral imaging system for characterizing vegetation spectral features, Comput. Electron. Agric. 63 (1) (2008) 13–21, http://dx.doi.org/10.1016/j.compag.2008.01.011, Special issue on bio-robotics.

[14] H. Tian, T. Wang, Y. Liu, X. Qiao, Y. Li, Computer vision technology in agricultural automation —A review, Inform. Process. Agric. 7 (1) (2020) 1–19, http://dx.doi.org/10.1016/j.inpa.2019.09.006.

[15] L. Costa, L. Nunes, Y. Ampatzidis, A new visible band index (vNDVI) for estimating NDVI values on RGB images utilizing genetic algorithms, Comput. Electron. Agric. 172 (2020) 105334, http://dx.doi.org/10.1016/j.compag.2020.105334.

[16] E. Fernández, G. Gorchs, L. Serrano, Use of consumer-grade cameras to assess wheat N status and grain yield, PLoS One 14 (2019) http://dx.doi.org/10.1371/journal.pone.0211889.

[17] J. Rasmussen, G. Ntakos, J. Nielsen, J. Svensgaard, R.N. Poulsen, S. Christensen, Are vegetation indices derived from consumer-grade cameras mounted on UAVs sufficiently reliable for assessing experimental plots? Eur. J. Agron. 74 (2016) 75–92, http://dx.doi.org/10.1016/j.eja.2015.11.026.

[18] S. Chung, L.E. Breshears, J.-Y. Yoon, Smartphone near infrared monitoring of plant stress, Comput. Electron. Agric. 154 (2018) 93–98, http://dx.doi.org/10.1016/j.compag.2018.08.046.

[19] A.R. Petach, M. Toomey, D.M. Aubrecht, A.D. Richardson, Monitoring vegetation phenology using an infrared-enabled security camera, Agricult. Forest Meteorol. 195–196 (2014) 143–151, http://dx.doi.org/10.1016/j.agrformet.2014.05.008.

[20] L. Shen, J. Su, R. He, L. Song, R. Huang, Y. Fang, Y. Song, B. Su, Real-time tracking and counting of grape clusters in the field based on channel pruning with YOLOv5s, Comput. Electron. Agric. 206 (2023) 107662, http://dx.doi.org/10.1016/j.compag.2023.107662.

[21] R.P. Devanna, A. Milella, R. Marani, S.P. Garofalo, G.A. Vivaldi, S. Pascuzzi, R. Galati, G. Reina, In-field automatic identification of pomegranates using a farmer robot, Sensors 22 (15) (2022) http://dx.doi.org/10.3390/s22155821.

[22] V. Sáiz-Rubio, F. Rovira-Más, Dynamic segmentation to estimate vine vigor from ground images, Spanish J. Agric. Res. 10 (3) (2012) 596–604, http://dx.doi.org/10.5424/sjar/2012103-508-11.

[23] M.A. Bourgeon, C. Gée, S. Debuisson, S. Villette, J.N. Jones, <<On-the-go>> multispectral imaging system to characterize the development of vineyard foliage with quantitative and qualitative vegetation indices, Precis. Agric. 18 (2017) 293–308, http://dx.doi.org/10.1007/s11119-016-9489-y.

[24] F. Crocetti, E. Bellocchio, A. Dionigi, S. Felicioni, G. Costante, M.L. Fravolini, P. Valigi, ARD-VO: Agricultural robot data set of vineyards and olive groves, J. Field Robotics 40 (6) (2023) 1678–1696, http://dx.doi.org/10.1002/rob.22179.

[25] Y. Yamasaki, M. Morie, N. Noguchi, Development of a high-accuracy autonomous sensing system for a field scouting robot, Comput. Electron. Agric. 193 (2022) 106630, http://dx.doi.org/10.1016/j.compag.2021.106630.

[26] A. Milella, R. Marani, A. Petitti, G. Reina, In-field high throughput grapevine phenotyping with a consumer-grade depth camera, Comput. Electron. Agric. 156 (2019) 293–306, http://dx.doi.org/10.1016/j.compag.2018.11.026.

[27] A. Ugenti, R. Galati, G. Mantriota, G. Reina, Analysis of an all-terrain tracked robot with innovative suspension system, Mech. Mach. Theory 182 (2023) 105237, http://dx.doi.org/10.1016/j.mechmachtheory.2023.105237.

[28] R. Galati, G. Mantriota, G. Reina, RoboNav: An affordable yet highly accurate navigation system for autonomous agricultural robots, Robotics 11 (5) (2022) http://dx.doi.org/10.3390/robotics11050099.

[29] U. Meier, Growth stages of mono-and dicotyledonous plants, second ed., in: BBCH Monograph, German Federal Biological Research Centre for Agriculture and Forestry, Berlin, 2001, http://dx.doi.org/10.5073/20180906-074619.

[30] M.A. Bourgeon, J.N. Paoli, G. Jones, S. Villette, C. Gée, Field radiometric calibration of a multispectral on-the-go sensor dedicated to the characterization of vineyard foliage, Comput. Electron. Agric. 123 (2016) 184–194, http://dx.doi.org/10.1016/j.compag.2016.02.019.